



HAL
open science

Characterization of fiber ultrashort pulse delivery for nonlinear endomicroscopy

A. Ibrahim, Fanny Poulon, R. Habert, Claire Lefort, Alexandre Kudlinski,
Darine Abi Haidar

► **To cite this version:**

A. Ibrahim, Fanny Poulon, R. Habert, Claire Lefort, Alexandre Kudlinski, et al.. Characterization of fiber ultrashort pulse delivery for nonlinear endomicroscopy. *Optics Express*, 2016, 24 (12), pp.12515-12523. 10.1364/OE.24.012515 . hal-01656576

HAL Id: hal-01656576

<https://hal.science/hal-01656576>

Submitted on 3 Jan 2018

HAL is a multi-disciplinary open access archive for the deposit and dissemination of scientific research documents, whether they are published or not. The documents may come from teaching and research institutions in France or abroad, or from public or private research centers.

L'archive ouverte pluridisciplinaire **HAL**, est destinée au dépôt et à la diffusion de documents scientifiques de niveau recherche, publiés ou non, émanant des établissements d'enseignement et de recherche français ou étrangers, des laboratoires publics ou privés.

Characterization of fiber ultrashort pulse delivery for nonlinear endomicroscopy

A. Ibrahim,¹ F. Poulon,¹ R. Habert,³ C. Lefort,⁴ A. Kudlinski,³ and D. Abi Haidar^{1,2,*}

¹Laboratoire IMNC, UMR 8165-CNRS, Orsay, France

²Université Paris 7-Paris DIDEROT, F-75013, Paris, France

³ Université Lille, CNRS, UMR 8523 - PhLAM - Physique des Lasers Atomes et Molécules, F-59000 Lille, France

⁴Laboratoire XLIM, UMR 7252, CNRS, F-87000 Limoges, France

*abihaidar@imnc.in2p3.fr

Abstract: In this work, we present a detailed characterization of a small-core double-clad photonic crystal fiber, dedicated and approved for *in vivo* nonlinear imaging endomicroscopy. A numerical and experimental study has been performed to characterize the excitation and collection efficiencies through a 5 m-long optical fiber, including the pulse duration and spectral shape. This was first done without any distal optics, and then the performances of the system were studied by using two kinds of GRIN lenses at the fiber output. These results are compared to published data using commercial double clad fibers and GRIN lenses.

©2016 Optical Society of America

OCIS codes: (190.0190) Nonlinear optics; (120.3890) Medical optics instrumentation; (120.3620) Lens system design; (060.2350) Fiber optics imaging; (130.3120) Integrated optics devices; (170.2150) Endoscopic imaging.

References and links

1. C. Odin, T. Guilbert, A. Alkilani, O. P. Boryskina, V. Fleury, and Y. Le Grand, "Collagen and myosin characterization by orientation field second harmonic microscopy," *Opt. Express* **16**(20), 16151–16165 (2008).
2. M. Monici, "Cell and tissue autofluorescence research and diagnostic applications," *Biotechnol. Annu. Rev.* **11**, 227–256 (2005).
3. S. Huang, A. A. Heikal, and W. W. Webb, "Two-photon fluorescence spectroscopy and microscopy of NAD(P)H and flavoprotein," *Biophys. J.* **82**(5), 2811–2825 (2002).
4. X. Jiang, J. Zhong, Y. Liu, H. Yu, S. Zhuo, and J. Chen, "Two-photon fluorescence and second-harmonic generation imaging of collagen in human tissue based on multiphoton microscopy," *Scanning* **33**(1), 53–56 (2011).
5. S. Zhuo, J. Chen, T. Luo, D. Zou, and J. Zhao, "Multimode nonlinear optical imaging of the dermis in ex vivo human skin based on the combination of multichannel mode and Lambda mode," *Opt. Express* **14**(17), 7810–7820 (2006).
6. C. Lefort, H. Hamzeh, F. Louradour, F. Pain, and D. A. Haidar, "Characterization, comparison, and choice of a commercial double-clad fiber for nonlinear endomicroscopy," *J. Biomed. Opt.* **19**(7), 076005 (2014).
7. H. Hamzeh, C. Lefort, F. Pain, and D. Abi Haidar, "Optimization and characterization of nonlinear excitation and collection through a gradient-index lens for high-resolution nonlinear endomicroscopy," *Opt. Lett.* **40**(5), 808–811 (2015).
8. H. Choi, S.-C. Chen, D. Kim, P. T. So, and M. L. Culpepper, "Design of a nonlinear endomicroscope biopsy probe," in *(Optical Society of America, 2006)*, p. Tu169.
9. F. Braud, T. Mansuryan, G. Ducourthial, R. Habert, A. Kudlinski, and F. Louradour, "Double clad photonic crystal fiber for high resolution nonlinear endomicroscopy," in *(OSA, 2014)*, p. SoW3B.2.
10. G. Ducourthial, P. Leclerc, T. Mansuryan, M. Fabert, J. Brevier, R. Habert, F. Braud, R. Batrin, C. Vever-Bizet, G. Bourg-Heckly, L. Thiberville, A. Druilhe, A. Kudlinski, and F. Louradour, "Development of a real-time flexible multiphoton microendoscope for label-free imaging in a live animal," *Sci. Rep.* **5**, 18303 (2015).
11. W. J. Wadsworth, R. M. Percival, G. Bouwmans, J. C. Knight, T. A. Birks, T. D. Hedley, and P. St. J. Russell, "Very High Numerical Aperture Fibers," *Photonics Technol. Lett. IEEE* **16**, 843–845 (2004).
12. C. Lefort, T. Mansuryan, F. Louradour, and A. Barthelemy, "Pulse compression and fiber delivery of 45 fs Fourier transform limited pulses at 830 nm," *Opt. Lett.* **36**(2), 292–294 (2011).
13. K. König, A. Ehlers, I. Riemann, S. Schenk, R. Bückle, and M. Kaatz, "Clinical two-photon microendoscopy," *Microsc. Res. Tech.* **70**(5), 398–402 (2007).
14. W. R. Zipfel, R. M. Williams, and W. W. Webb, "Nonlinear magic: multiphoton microscopy in the biosciences," *Nat. Biotechnol.* **21**(11), 1369–1377 (2003).
15. H. Bao, A. Boussioutas, R. Jeremy, S. Russell, and M. Gu, "Second harmonic generation imaging via nonlinear endomicroscopy," *Opt. Express* **18**(2), 1255–1260 (2010).

1. Introduction

Two-Photon Microscopy (TPM) has become a standard technique extensively used for imaging optically thick biological tissues [1]. It is able to provide a wealth of information about specific structures without exogenous fluorescent labels. This performance is achieved through various endogenous contrasts: (1) Second Harmonic Generation (SHG), to highlight specific elements, such as myosins and collagens [1], and (2) fluorescence under two photon excitation (TPE), to investigate endogenous fluorophores, such as reduced nicotinamide adenine dinucleotide (NADH) and Flavin, a well-known biomarkers of cellular energy metabolism [3,4]. TPM provide intrinsic sectioning, lack of out-of-focus photobleaching, a localized phototoxicity, important penetration depth due to decreased scattering from long infrared excitation wavelengths and absence of overlapping between excitation and emission. Despite these advantages, the TPM is still limited to laboratory thick tissues testing. Currently, its main applications are focused on fixed or ex vivo samples and in vivo tests are limited to animals. The systems available nowadays to image in vivo human tissues are macroscopic and can only be applied at the skin level [4,5]. A more dedicated solution to study in vivo and in situ human tissues could be nonlinear endomicroscopy. It presents the advantages of TPM and gives the possibility to an in vivo and in situ tissues imaging without resorting to a surgical biopsy, thanks to the use of a thin and elongated optical fiber coupled with miniaturized objective lens instead of the microscope objective. It allows less invasive tests and earlier detection of diseases.

The development of such nonlinear endomicroscopic systems requires a specific attention to the choice of the endoscopic fiber. It should be able to preserve the temporal confinement of short pulses that need to be delivered to the distal optics for different excitation wavelengths. For that, dispersion pre-compensation schemes are usually employed. This fiber should also have a small core diameter to reach high imaging resolution via miniaturized optics as well as a high inner cladding numerical aperture (NA) to be able to collect endogenous weak fluorescence signals. This is usually done using so-called double-clad fibers (DCFs).

By referring to the literature, and to our previous study, different commercially available DCFs were compared and characterized with and without miniaturized objective [6,7]. The DCF DC-165-16-P from NKT Photonics [8], a microstructured fiber, turned out to be the best in terms of single-mode delivery of ultrashort pulses around 800 nm. However, its core diameter (around 16 μm) is a real problem for the miniaturization of the distal optic. The resulting optical resolution is inevitably altered and worse, compared to a DCF with a smaller core but a doped inner cladding, such as the Fibercore SMM900. Based on these results we were convinced that the ideal fiber did not exist yet. Consequently, it was necessary to conceive a specific DCF combining a small and undoped silica core with a high inner cladding numerical aperture (NA). Such a fiber will deliver high-quality excitation pulses with a low level of optical aberrations in the distal optics, and the highest level of nonlinear signal collection with miniaturized optical lenses. Such a small-core double-clad photonic crystal fiber (DC-PCF), specially designed for the two-photon endomicroscope, has been published recently in the context of the development of an endomicroscope [9,10]. This fiber was able to achieve efficient non-linear endomicroscope images.

This work represents a continuity of our previous studies based on characterization of commercial DCFs [6,7]. Here we extend it to the very recently introduced small-core double-clad photonic crystal fiber (DC-PCF) joined to different GRIN lenses [9,10]. We provide a full characterization of the output short pulse properties and collection efficiency from a scattering sample for input pulse duration in the range 100-300 fs and wavelength of 750-900 nm as a function of pump power, showing efficient femtosecond pulse delivery of the system made of the DC-PCF coupled to a GRISM pre-compensation scheme and GRIN lenses over this whole range of parameters.

2. Materials and methods

2.1. Customized DC-PCF design

This customized DC-PCF is shown in Fig. 1(a) and 1(b). The hole-to-hole spacing and relative hole diameter are respectively $3.5\mu\text{m}$ and 0.41 . The central core has a diameter of $6.4\mu\text{m}$ and is single-mode at 800 nm . It is surrounded by an air/silica microstructured region of $40\mu\text{m}$ diameter. The DC-PCF used here is 5 m -long, which is 5 times longer than commercial fibers typically used for the same purpose. The NA of the small core at 800 nm is 0.097 , the second order dispersion coefficient is $\beta_2 = 2.9 \times 10^{-26}\text{ s}^2/\text{m}$ and the nonlinear parameter is $\gamma = 10.5\text{ W}^{-1}\cdot\text{km}^{-1}$ at this wavelength. The fiber presents a second microstructure (ring of large air holes) to separate the collecting inner cladding from the outer maintaining cladding. The size of the bridge between the air holes will determine the NA of the inner cladding: the smaller is the bridge, the higher is the numerical aperture [11]. Here the thickness of silica bridges between air holes is around 500 nm , and the NA of the inner cladding was measured to be 0.27 at 450 nm . This fiber regroups the advantages of a microstructured fiber, by using an undoped core to avoid autofluorescence, but has a smaller core diameter than the NKT Photonics DCF, giving a better axial and lateral resolution.

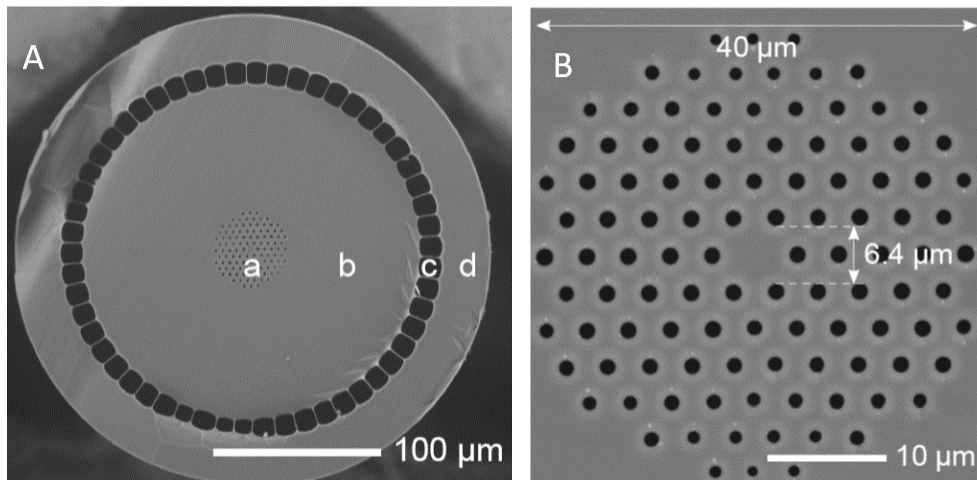


Fig. 1. A. Scanning electron microscope image of the DC PCF. a) Core region surrounded by an air-silica microstructure b) Collecting cladding c) Low index air cladding d) Maintaining cladding. B. Details of the air-silica microstructure around the core.

2.2. Setup design for ultra-short pulse delivery characterization

The architecture of the proposed endomicroscope, presented in Fig. 2, is composed of a femtosecond titanium sapphire oscillator (Ti:Sa, Mai Tai DeepSee, eHP, Spectra physics). A Faraday Isolator (FI), placed at the laser output, avoids back reflection from the fiber input face and destabilization of the pulse in the laser cavity.

A pre-compensation unit is used to compensate dispersion (second and third orders simultaneously) and nonlinear effects (mainly self-phase modulation) appearing inside the endoscopic fiber [10]. This unit is composed of a first polarization-maintaining single mode fiber (SMF) (0.5 m) used to broaden the spectrum in order to be able to reach a shorter pulse duration afterwards [12]. It is followed by a GRISM-based anomalous stretcher, consisting in the assembly of a diffraction grating with a prism [6,7,12]. Pulses are then coupled into the endoscopic DC-PCF. It allows simultaneous excitation by the small core and fluorescence collection from the tissue by the inner cladding. The focusing of the light in the specimen is achieved using a specific miniature GRIN lens. The response through the 5 m -long DC-PCF

and the GRIN lenses was characterized spectrally and temporally using respectively a spectrometer (FLAME-S-VIS-NIR-ES 1, Ocean optics spectrometer, France) and an autocorrelator (Mini-PMT-NIR, AA11.08.01.03, APE). Two different pulse durations were set at the output of the laser cavity using the Deepsee system. The first one, around 300 fs, is a pulse duration used classically in nonlinear microscopy. The second one, around 100 fs, is close to the optimal pulse duration obtained when using a Deepsee after the laser oscillator.

This DC-PCF has been made to excite the sample and collect fluorescence signals at the same time, using a dichroic mirror, Fig. 2. Laser light goes through the GRIN lens to be focalized on the sample (Rhodamine) insuring maximum excitation. Fluorescence emitted by the Rhodamine is detected by the second core of the DC-PCF and lead through the dichroic mirror to the spectrometer (QE Pro, Ocean optics spectrometer, France).

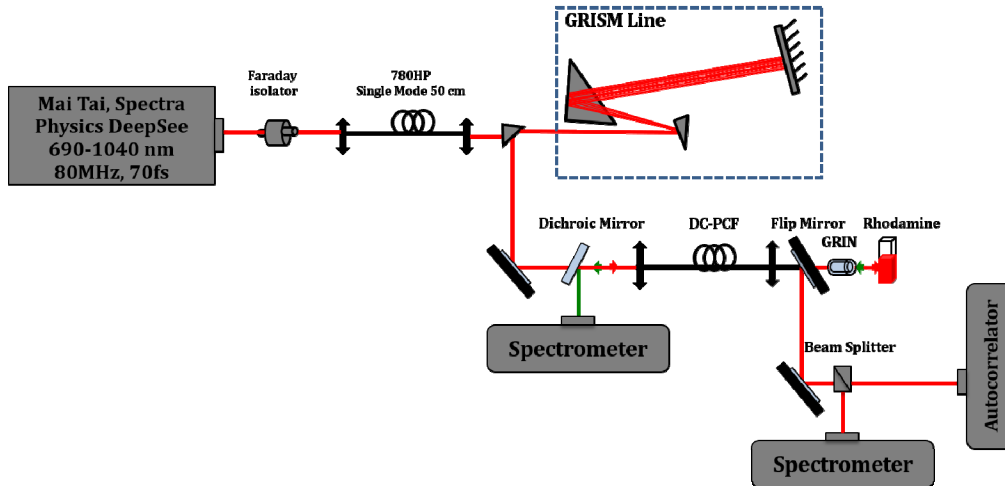


Fig. 2. Experimental setup.

2.3. GRIN lenses

Two different GRIN lenses adapted to wavelengths between 800 and 900 nm were used. The first one (GRIN 1) coded GT-MO-080-018-810 has a 1.4 mm diameter. It is a complex optical system with a spherical lens and two GRIN lenses fabricated with a special gradient profile. Its object space NA is 0.8, and the image space NA is 0.18. The total length of this lens is 7.53 mm. In the second lens (GRIN 2) coded GT-MO-080-0415-810, the image space NA is 0.4 and the length is 4 mm. Both GRINs, fabricated by GRINTECH, are mounted in stainless steel tubing. The differences in the image space NA could affect the collection of the fiber output signal. The difference in length could also affect dispersion and pulse duration.

3. Results

3.1 Efficient excitation using the DC-PCF fiber for different excitation wavelengths and cavity output pulse duration

Two different pulse durations were set at the output of the laser cavity using the Deepsee system. The first one, around 300 fs, is a pulse duration used classically in nonlinear microscopy. The second one, around 100 fs, is close to the optimal pulse duration obtained when using a Deepsee after the laser oscillator. These two extreme durations allow us to estimate the capacity of our system to optimize the pulse at the output of the endoscopic fiber. These measurements were performed for different excitation wavelengths from 750 to 900 nm. The temporal measurements to characterize the fiber and the two GRINs are summarized in Table 1. At each wavelength, the GRISM line mentioned above was optimized in order to get the shortest pulse duration at the output of the system. The pulse duration is obtained by

measuring the full width at half maximum (FWHM) from the autocorrelator data using a Gaussian profile for the deconvolution.

For a pulse duration of 300 fs at the output of the laser cavity, the shortest pulse duration at the output of the endoscopic fiber is approximately 42 fs for a 810 nm excitation wavelength. This value decreases to 33 fs with a laser output cavity pulse at 100 fs, presented in Fig. 3(b). Moreover, by fixing the laser pulse duration at the output of the cavity to 100 fs, we notice that the difference between the shortest and the longest pulse duration at the output of the DC-PCF is 72 fs at the different wavelength, while for a 100 fs laser pulse duration the difference is only 27 fs. The variability of the output pulse duration of the system especially for 100 fs cavity pulse duration is low, highlighting the tenability of our setup. This point is especially important in the context of *in vivo* endogenous fluorescence imaging which frequently requires the use of different excitation wavelengths depending upon the tissue nature.

Table 1. Measured Pulse Duration at the Output of the Endoscopic Fiber Alone, with Grin 1 and with Grin 2 for Different Laser Cavity Pulse Durations

	Laser Cavity output pulse at 300 fs			Laser Cavity output pulse at 100 fs		
	DC-PCF	DC-PCF + G1	DC-PCF + G2	DC-PCF	DC-PCF + G1	DC-PCF + G2
750 nm	72 ± 3,6	84 ± 4,2	80 ± 4	60 ± 3	70 ± 3,5	65 ± 3,25
780 nm	69 ± 3,45	76 ± 3,8	74 ± 3,7	55 ± 2,75	62 ± 3,1	59 ± 2,95
800 nm	45 ± 2,25	65 ± 3,25	63 ± 3,15	33 ± 1,65	50 ± 2,5	45 ± 2,25
810 nm	42 ± 2,1	53 ± 2,65	51 ± 2,55	33 ± 1,65	42 ± 2,1	40 ± 2
860 nm	64 ± 3,2	75 ± 3,75	87 ± 4,35	49 ± 2,45	58 ± 2,9	58 ± 2,9
890 nm	85 ± 4,25	136 ± 6,8	93 ± 4,65	55 ± 2,75	75 ± 3,75	70 ± 3,5
900 nm	114 ± 5,7	150 ± 7,5	105 ± 5,25	58 ± 2,9	90 ± 4,5	78 ± 3,9

3.2 Coupling GRINs lenses to the DC-PCF

Two conditions are required for nonlinear absorption: spatial and temporal confinement of the excitation pulses. Temporal confinement is obtained thanks to the optimal adjustment of the GRISM line, compensating simultaneously for the second and the third orders of dispersion of the endoscopic system. For spatial confinement, this new fiber was also coupled with GRIN lenses. By that, spatial and temporal confinements of the excitation are acquired for efficient nonlinear excitation. Consequently, imaging of tissues with a high resolution is expected. The GRIN lens with a radial refractive index and a high numerical aperture (NA) has been already validated for clinical use [13] due to their flat surface and small diameter.

Since the 100 fs laser pulses give the best performances as shown above, we chose to analyze the effect of the GRIN lenses on the pulse duration at the endoscopic system output with this laser setup. Adding respectively GRIN1 or GRIN2 at the DC-PCF output affects marginally the response of the pulse duration. For example, at 810 nm, we have the pulse duration values of 33 fs, 42 fs, and 40 fs respectively for the DC-PCF alone, the DC-PCF coupled to the GRIN1 and the DC-PCF coupled to the GRIN2. This difference of 24% or 19% between the fiber alone and the fiber coupled to GRIN 1 or 2 is due to the two distinct dispersion characteristics of these two GRIN lenses. This means that adding GRIN lenses do not affect the pulse duration confinement significantly; subsequently excitation quality is not affected. These results are also highlighted in Fig. 3(c).

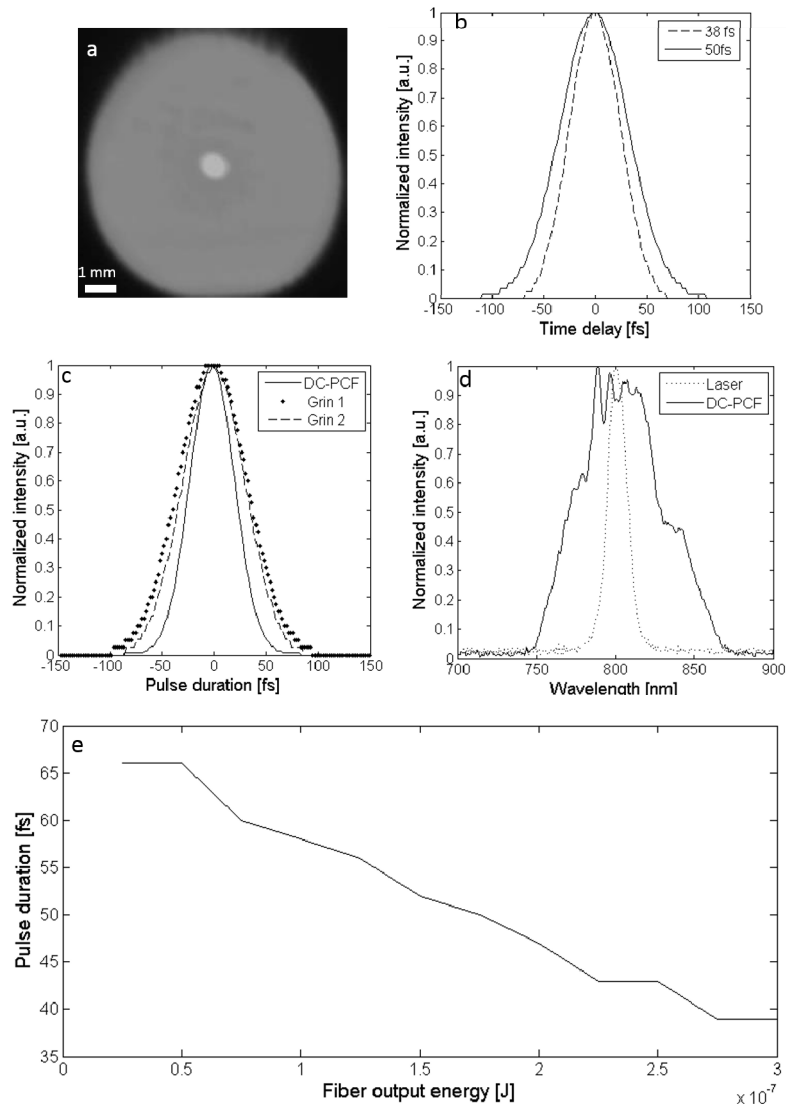


Fig. 3. The laser excitation is set to 800 nm (a) Delivery of the fundamental mode of the light after adjusting the collimation at the first fiber output. (b) The autocorrelation duration of the pulse at the output of DC-PCF obtained by adjusting the laser pulse duration respectively at 300 fs and 100 fs. (c) The optimal pulse duration obtained without GRIN and with GRIN 1 and GRIN 2. (d) Spectral characterization of the laser output and PhLAM fiber output. For these measurements, the wavelength and output power used were 800 nm and 20 mW (e) Pulse duration variation as a function of fiber output.

Experimentally, GRIN 2 gave a slight advantage in pulse duration compared to GRIN 1 at each wavelength, on average 7% shorter for GRIN 2, except at 860 nm where the pulse duration was the same. The spectral analysis performed on the short pulse throughout the setup is shown in Fig. 3(d). This figure presents the spectral shape at the laser cavity and the DC-PCF output. The DC-PCF output spectrum is wider than at the output of the laser thanks to the shaping module before the endoscopic fiber. This allows to obtain shorter compressed pulses. Figure 3(e) shows the variation of the DC-PCF pulse duration at the core with the laser operating at mean power. In the range from 2 mW to 24 mW, we note a reduction of pulse duration with higher power, from 66 fs at 2 and 4 mW, to 39 fs at 22 and 24 mW.

The DC-PCF was also compared numerically to the best commercial DCF presented in our previous study [7]. These numerical tests were performed with a Zemax (Optics Studio 14.2, Zemax LLC) simulation. The DC-PCF was coupled to two different GRIN lenses. The first one was a custom designed (GT-IRLS-050-11-50-NC) in order to be compared with our results previously published results [7], and the second one was the commercial GRIN 1 (GT-MO-080-018-810) used in the experimental measurements. The axial and lateral resolutions of the coupling of the fiber into these GRINs were characterized. These two parameters were computed in accordance with a method taken from the literature [14]. It represents the resolution at the FWHM, calculated from the spot in the focal plane of the GRIN, using a Gaussian beam approximation to simulate the output of the fiber and the propagation through the optics. The results are summarized in Table 2. The DC-PCF has a lateral resolution 2.5 times higher than the NKT Photonics DCF, and is 5-6 times better regarding the axial resolution, and only slightly less resolved than the Fibercore one (1.8 times less resolved).

Table 2. Resolution of the Excitation Spot in the Focal Plan of the Two GRIN Lenses Coupled to Our Fiber

Fiber	Core-Cladding diameter (μm)	Core NA	Homemade GRIN			GRIN-GT-MO-080-018-810		
			Lateral resolution (μm)	Axial resolution (μm)	Waist size (μm)	Lateral resolution (μm)	Axial resolution (μm)	Waist size (μm)
Fibercore (SMM900)	3.6-100	0.19	0.22	0.33	0.26	0.32	0.80	0.38
Crystal Fiber (DC-165-16P)	16-163	0.04	1.00	7.99	1.20	1.44	16.61	1.73
DC-PCF (T904B)	6.4-268	0.097	0.40	1.28	0.48	0.58	2.67	0.69

3.3 Fluorescence collection efficiency using the DC-PCF

As explained in the introduction, the ability of a DCF to be used as an endoscopic fiber not only depends on its excitation properties, but also on its ability to collect the signal emitted by samples. The collection efficiency depends on the size of the DCF inner cladding (second core) and of its NA. The influence of the pulse duration and average power on the fluorescence emission level is analyzed here using Rhodamine as fluorescent solution. Fluorescent signal emitted by Rhodamine was characterized as a function of (i) the duration of the excitation pulse at the output of the DC-PCF, Fig. 4(a), and (ii) the output average beam power while the pulse duration is kept constant, Fig. 4(b). In this part, we used 1mM of rhodamine placed after the GRIN 2 lens. First we set the beam power at 14 mW at the focal volume, and we changed the pulse duration. We note that the fluorescence signals decrease by increasing pulse duration, but they were still detected until 330 fs, Fig. 4(a). This experiment confirms the importance of using short pulse duration to enhance the fluorescent signal. In second time, we set the pulse duration to 60 fs and we increase the power beam from 1 mW to 20 mW on focal volume. Note that 20 mW is more than sufficient for exciting endogenous fluorophores of tissues. This fiber is not autofluorescent and that was confirmed by measuring the collected fluorescence without sample at the output of the system. This measurement is defining the level of dark current and is not changing when increasing the power. We note that the fluorescence signals emitted decrease by decreasing the beam excitation power, Fig. 4(a). The variation of the excitation power, for fixed pulse duration, shows that it could be possible to reach 40 mW at the output of the DC-PCF while keeping the same spectral shape and without expecting autofluorescence from the fiber.

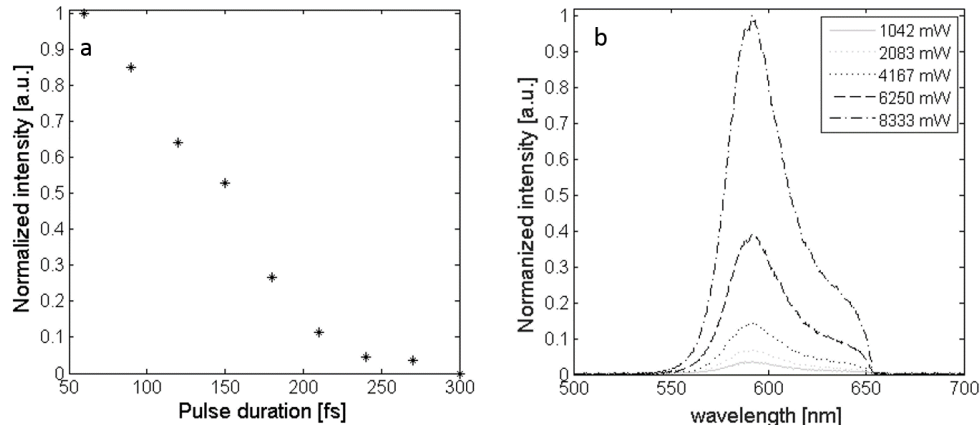


Fig. 4. Backward TPF from Rhodamine with the DC-PCF (a) Fluorescence intensity as a function of the DC-PCF and GRIN output pulse duration, normalized to the TPF intensity at 60 fs, (b) Rhodamine TPF as a function of the pulse peak power at DC-PCF output.

3.4 Transmission of the DC-PCF on a wide spectral range

In the majority of the cases, the endoscopic imaging requires to use various excitation wavelengths according to the aim of the study, and especially if based on the analysis of the endogenous molecules. Even when the excitation wavelength is fixed, various endogenous molecules can emit. To verify if this fiber is optimal for a wide range of excitation wavelength or for the collection of the emitted fluorescence by different molecules, a specific study is needed. For this, a spectral lamp (HPX-2000 Family, Ocean Optics, France) was used as sample. For this purpose, a monochromator devices was used to select wavelengths of this spectral lamp. The beam was collected at the output of this monochromator (Scanning Monochromator MonoScan2000, Ocean, Optics, France) and injected in the inner cladding of the DC-PCF. The beam power was measured at the input and output of this fiber to calculate the transmission coefficient every time we change the wavelength. The transmission from different wavelength and at a fixed fiber - sample distance was measured in order to define the transmission coefficient. Results prove that this fiber is able to collect different wavelength ranging from 200 to 1000 nm). We do not have an important variation in transmission coefficient except around wavelengths 340 nm and 850 nm, which presented the maximum of transmission coefficient.

4. Discussion and conclusion

A new double-clad photonic crystal fiber for nonlinear imaging has been presented and characterized experimentally and numerically. First, by using the shortest pulse possible at the laser cavity output, combined to a GRISM line, we were able to reach a pulse duration of 33 fs at the output of a 5 m endomicroscopic customized fiber without a miniaturized GRIN lens, and 40 fs at the output of the fiber coupled to a miniaturized GRIN lens. These values represent significant improvements over previously reported two-photon imaging that up to now have been restricted to picosecond pulses [15]. Obviously, we can fix the pulse compression to around 100 fs. In the future, we envisage making a study, which will allow us to estimate the potential benefits of these extremely short pulse durations for tissue imaging. This homemade fiber is 5-meters-long, which is appreciably much longer than the 1-meter-long commercial DCF usually tested in endomicroscopy setups. We have demonstrated that our setup is able to compensate for the dispersion through such long fibers, and to provide pulses as short as those obtained with 1-meter-long fibers. This presents a real advantage in medical imaging applications, indeed a 5-meters-long fiber will allow the placement of the optical head in the operating room, while the laser and compression system can be kept

outside in a non-sterilized environment. Secondly, by comparing our results to those previously reported [6] using a DCF, we note that in our case the spectral broadening after the DC-PCF is approximately the same. With this spectral large band, we hope to be able to excite different endogenous molecules. Thirdly, in order to ensure the coherence in our imaging studies, we can adjust our system in such a way as to minimize pulse duration variation when the excitation wavelength is changed. In addition, for all possible excitation wavelengths, we can obtain pulse durations shorter than 60 fs at the output of our DC-PCF by using laser pulse duration of 100 fs. This ensures a temporal confinement required for an optimal nonlinear excitation. The collection efficiency was measured for different pulses duration showing the importance of using short pulses when we expect tissue imaging. For a fixed pulse duration, experimental results show the enhancement of fluorescence signal with excitation power.

Finally, this new fiber coupled to a GRIN lens has a significantly better simulated resolution than other microstructured DCF (NKT Photonics DC-165-16 P) used in literature for endoscopic imaging and is not far from the performance of the best commercial DCF either, the Fibercore SMM900. Moreover, our fiber delivered shorter pulses than those generated by the Fibercore one [6], thus showing that the new DC-PCF has the advantages of an undoped core fiber, no risk of parasite autofluorescence, while maintaining an acceptable resolution for imaging with the same pulse duration performance.

The influence of the pulse duration and average power on the fluorescence collection was analyzed. We note that the fluorescence signals decrease by increasing pulse duration, but they were still detectable until 330 fs. The fluorescence signals emitted decrease by decreasing the beam excitation power.

Indeed the critical resolution with deep tissue imaging is the axial resolution, it has to be smaller than the characteristic size of the observed sample in order to have a sharp image and achieve z sectioning, here for the DC-PCF the axial resolution is about 1.5 μm and the smallest characteristic size we observe in our biopsy sample, using a classical two-photon microscope, is approximately 10 microns. Finally, the characterization of the excitation and collection path through the DC-PCF shows that we found the homemade architecture to answer our technical specifications.

Acknowledgments

This Work as a part of the MEVO project was supported by “Plan Cancer” program founded by INSERM (France), by CNRS with “Défi instrumental” grant, and the Institut National de Physique Nucléaire et de Physique des Particules (IN2P3). This work was done in the PIMPA Platform partly funded by the French program “Investissement d’Avenir” run by the “Agence Nationale pour la Recherche” (grant “Infrastructure d’avenir en Biologie Santé – ANR – 11-INBS-0006”). Co-authors from PhLAM acknowledge support from the “Fonds Européen de Développement Economique Régional”, the Labex CEMPI (ANR-11-LABX-0007) and Equipex FLUX (ANR-11-EQPX-0017) through the “Programme Investissements d’Avenir”. We warmly thank James M. Ablett from Synchrotron SOLEIL for valuable discussion.